Boise State University
ScholarWorks

Geosciences Faculty Publications and Presentations

Department of Geosciences

8-1-2013

High-Resolution $\delta^{13}C_{carb}$ Chemostratigraphy from Latest Guadalupian Through Earliest Triassic in South China and Iran

Vladimir Davydov
Boise State University

NOTICE: This is the author's version of a work that was accepted for publication in *Earth and Planetary Science Letters*. Changes resulting from the publishing process, such as peer review, editing, corrections, structural formatting, and other quality control mechanisms may not be reflected in this document. Changes may have been made to this work since it was submitted for publication. A definitive version was subsequently published in *Earth and Planetary Science Letters*, 375 (1 Aug 2013). DOI: 10.1016/j.epsl.2013.05.020.

This is an author-produced, peer-reviewed version of this article. The final, definitive version of this document can be found online at *Earth and Planetary Science Letters*, published by Elsevier. Copyright restrictions may apply. DOI: 10.1016/j.epsl.2013.05.020.

High-resolution $\delta^{13}c_{carb}$ chemostratigraphy from latest Guadalupian through earliest Triassic in south China and Iran

Shu-zhong Shen*
State Key Laboratory of Paleobiology and Stratigraphy
Nanjing Institute of Geology and Palaeontology
39 East Beijing Road
Nanjing 210008, China

Chang-qun Cao
State Key Laboratory of Paleobiology and Stratigraphy
Nanjing Institute of Geology and Palaeontology
39 East Beijing Road
Nanjing 210008, China

Hua Zhang
State Key Laboratory of Paleobiology and Stratigraphy
Nanjing Institute of Geology and Palaeontology
39 East Beijing Road
Nanjing 210008, China

Samuel A. Bowring
Department of Earth, Atmospheric and Planetary Sciences
Massachusetts Institute of Technology
77 Massachusetts Avenue
Cambridge, MA 02130, USA

Charles M. Henderson
Department of Geoscience
University of Calgary
Calgary, AB, Canada T2N 1N4

Jonathon L. Payne
Department of Geological and Environmental Sciences
Stanford University
Stanford, CA94305, USA

Vladimir I. Davydov
Department of Geosciences
Boise State University
1910 University Drive
Boise, ID 83725, USA

Dong-xun Yuan
State Key Laboratory of Paleobiology and Stratigraphy
Nanjing Institute of Geology and Palaeontology
39 East Beijing Road
Nanjing 210008, China

Yi-chun Zhang
State Key Laboratory of Paleobiology and Stratigraphy
Nanjing Institute of Geology and Palaeontology
39 East Beijing Road
Nanjing 210008, China

Wei Wang
State Key Laboratory of Paleobiology and Stratigraphy
Nanjing Institute of Geology and Palaeontology
39 East Beijing Road
Nanjing 210008, China

This is an author-produced, peer-reviewed version of this article. The final, definitive version of this document can be found online at *Earth and Planetary Science Letters*, published by Elsevier. Copyright restrictions may apply. DOI: 10.1016/j.epsl.2013.05.020.

ABSTRACT

Large carbon cycle perturbations associated with the end-Permian mass extinction and subsequent recovery have been widely documented, but Late Permian (Lopingian) carbon cycle dynamics prior to the mass extinction event remain poorly documented. Here we present a high-resolution $\delta^{13}C_{carb}$ chemostratigraphic framework from latest Guadalupian to earliest Triassic time, calibrated with high-resolution conodont biostratigraphy and high-precision geochronology. We observe two large negative excursions in $\delta^{13}C_{carb}$, the first in uppermost Guadalupian strata and the second at the end of the Changhsingian stage, and between these events distinctive excursions from the middle Wuchiapingian to the early Changhsingian. The end-Changhsingian excursion represents a major reorganization of the global carbon cycle associated with the end-Permian mass extinction. However, the extent to which the end-Guadalupian and Wuchiapingian/Changhsingian boundary excursions result from local versus global controls remains unresolved. Regardless of their underlying causes, these three excursions provide chemostratigraphic markers for global correlation of Lopingian strata.

Keywords: Lopingian, $\delta^{13}C_{carb}$ chemostratigraphy, south China, Iran, correlation

INTRODUCTION

The largest mass extinction event during the Phanerozoic was associated with a major perturbation to the global carbon cycle that is recorded in the stable carbon isotope ratios of sedimentary rocks and fossils. Rapid large negative isotope excursions in the $\delta^{13}C$ of both carbonate rocks ($\delta^{13}C_{carb}$) and organic matter ($\delta^{13}C_{org}$) occurred globally within the interval immediately below the Permian-Triassic boundary (PTB) (see a review by Korte and Kozur, 2010) and have been interpreted to result from widespread volcanism in Siberia and south China (e.g., Shen et al., 2012) and/or associated massive carbon release from sedimentary strata or methane clathrates (Retallack and Jahren, 2008; Svensen et al., 2009). The main pulse of the end-Permian mass extinction occurred in less than 200 Kyr based on high-resolution biostratigraphic, chemostratigraphic, and radioisotopic data from south China (Shen et al., 2011).

Carbon isotope variations across the PTB have been extensively documented and numerous records now document the large carbon isotope excursions that persist in the Lower Triassic strata as well (e.g., Horacek et al., 2007; Payne et al., 2004; Tong et al., 2007). However, the carbon isotope record for the Lopingian remains poorly documented prior to the end-Permian extinction interval. Consequently, it is unclear whether the end-Permian and Early Triassic carbon cycle perturbations occurred against a background of long-term stability or, rather, represent the continuation of Late Permian carbon cycle instability. In this paper, we attempt to fill this knowledge gap by documenting the C-isotope compositions of marine bulk carbonate samples spanning the uppermost Guadalupian through the lowest Triassic from four sections in south China through the high-resolution biostratigraphy correlations to the sections in Iran (Fig. 1).

This is an author-produced, peer-reviewed version of this article. The final, definitive version of this document can be found online at *Earth and Planetary Science Letters*, published by Elsevier. Copyright restrictions may apply. DOI: 10.1016/j.epsl.2013.05.020.

SECTIONS AND MATERIALS

South China and Iran were situated in the vast, semi-enclosed Palaeotethys Ocean during Lopingian time and contain continuous carbonate deposits with highly diverse faunas. Furthermore, the sections in south China also contain volcanic ash layers; they are, therefore ideal areas for high-resolution biostratigraphic (Kozur, 2005; Shen and Mei, 2010), chemostratigraphic (Cao et al., 2009; Korte et al., 2004a; Richoz, 2006; Shen et al., 2010) and geochronologic (Shen et al., 2011) studies in order to constrain various Lopingian events. Herein, we report data from four sections in south China, which form a series from shallow-to deep-water depositional environments, and four sections from Iran, two of which are newly-studied (Figs. 1-3). We used these sections to develop a carbon isotope record spanning the entire Lopingian calibrated by high-resolution biostratigraphy and geochronologic ages.

South China

The Lopingian Series at the Matan section in Heshan of Guangxi Province, south China, overlies the Late Guadalupian Maokou Formation and consists of the Heshan and Talung formations. The Heshan Formation was deposited on a shallow water carbonate platform under a warm and humid climate. It grades laterally into nearshore peat flat facies and coastal lagoon facies (2003). The overlying Talung Formation at the Matan sectionis represented by submarine fan turbidite facies deposited in a deep-water basin. It contains abundant volcaniclastic layers in the upper Changhsingian.

The stratotype section at Meishan with two GSSPs is one of the most intensively studied sections in terms of the end-Permian mass extinction. However, strata below the WCB are not exposed at the Meishan quarries. A drilling project at Meishan recovered fresh core samples to develop a detailed carbon isotope profile reaching down into the interval about 50 m below the WCB. The deepest part of the core in the late Wuchiapingian Lungtan Formation is dominated by organic-rich mudstone, shale, siltstoneand sandstone; therefore, $\delta^{13}C_{carb}$ analysis was not possible.

The Shangsi section in Guangyuan, Sichuan Province, is another well-studied section in terms of the end-Permian mass extinction (Li et al., 1989; Mundil et al., 2004; Riccardi et al., 2007; Shen et al., 2011). This section consists of deep-water facies. The Lopingian Series is composed of the dark carbonate Wuchiaping Formation in the lower and the siliceous carbonate or cherty Talung Formation in the upper part. Both formations are rich in organic matter and contain abundant ammonoids and conodonts.

The Dukou section in Xuanhan, Sichuan Province, is a carbonate platform sequence. The Lopingian Series is composed of dark limestone containing abundant conodonts (Mei et al., 1994a; 1994b) and fusulinds interbedded with chert or cherty nodules, and is topped with a very thick dolomitic limestone unit near the PTB.

Iran

The Lopingian sequence at Kuh-e-Alibashi in NW Iran is mostly composed of grayish pelagic carbonates interbedded with thick mudstone of the Julfa Beds and the reddish carbonate Alibashi Formation (Teichert et al., 1973). The Wuchiapingian Julfa beds contain abundant benthic fossils indicating a normal shallow marine environment in the lower part that is called the *Araxilevis* Bed. The upper part of the Julfa beds and the

This is an author-produced, peer-reviewed version of this article. The final, definitive version of this document can be found online at *Earth and Planetary Science Letters*, published by Elsevier. Copyright restrictions may apply. DOI: 10.1016/j.epsl.2013.05.020.

overlying Alibashi Formation are composed of thin-bedded gray or reddish limestone containing abundant ammonoids and conodonts with rare benthic fossils, and therefore have been interpreted to represent a pelagic facies (Kozur, 2004; 2005; Teichert et al., 1973). The conodont zones recently refined by Kozur (2004; 2005) and Shen and Mei (2010) enable a high-resolution biostratigraphic correlation of Lopingian strata between south China and Iran. The Permian sequence at the Abadeh section in central Iran consists of the Abadeh, Hambastand Elikah formations in ascending order, a sequence largely comparable with that at Kuh-e-Alibashi in NW Iran.

RESULTS AND COMPARISONS

Lopingian C-isotope profiles from south China and Iran are respectively shown in Figures 2 and 3. Detailed carbon isotope data, methods and an analysis of correlation between carbon and oxygen isotopes are presented in data repository. The high-resolution conodont zones and U-Pb ash bed geochronology enable precise correlations of the $\delta^{13}C_{carb}$ excursions among sections. We recognize three primary excursions.

The end-Guadalupian negative excursion

Distinct positive shifts in $\delta^{13}C$ between 4-8‰ around the GLB occur in the sections from south China (Figs. 2, 4). A negative shift of 4‰ occurs 3 m below the GLB at the Shangsi section, followed by a gradual positive shift to the *Clarkina dukouensis* Zone. A sharp positive shift of about 4.4‰ occurs in the interval between 7.8 m below the GLB and 3.5 m above the GLB at Matan, Heshan. This sharp positive excursion around GLB suggests some strata (e.g., *Jinogondolella granti*, *Clarkina postbitteri* zones) in the topmost Guadalupian may be absent or the interval with the negative shift is represented by the Wangpo carbonaceous shale at the both Shangsi andMatan sections. A larger positive excursion of about 7‰ from the latest Guadalupian to the early Wuchiapingian *Clarkina dukouensis* Zone occurs at the Dukou section. This excursion begins in a horizon about 10 m below the GLB and increases from-2.3‰ to +4.8‰ at the GLB (Fig. 2).

C-isotope profiles around the GLB in other areas vary in pattern and magnitude of isotopic shifts. Chemostratigraphy from the Lopingian-base GSSP section at the Penglaitan and Tieqiao sections in Guangxi Province (Jin et al., 2006; Wang et al., 2004) shows $\delta^{13}C$ values that drop from +2.0‰ in the Laibin Limestone (*Jinogondolella granti* Zone) to -0.7‰ at the base of the Heshan Formation in the upper part of the *Clarkina postbitteri postbitteri* Subzone of the Tieqiao section, before recovering to an average+4.3‰ value in Unit 9 (Wang et al., 2004). This pattern has been confirmed by subsequent studies from the nearby Penglaitan GSSP section (Chen et al., 2011; Kaiho et al., 2005), but no large negative shift of $\delta^{13}C$ in the Late Guadalupian was detected (Chen et al., 2011). The pattern is different from that documented by Wignall et al. (2012; 2009). A large negative shift of *ca.* 6‰ reported from the *Jinogondolella xuanhanensis* Zone in Guizhou; but is not confirmed at the Penglaitan section in south China (Chen et al., 2011; Kaiho et al., 2005; Wang et al., 2004) and the sections in Hungary and Greece (Wignall et al., 2012).

Our results indicate that the negative excursion of *ca.* 4‰ at the Matan and Shangsi sections and 7‰ at the Dukou section from the topmost part of the Maokou Formation (Late Capitanian) to the basal Wuchiapingian are more or less similar to that reported from Guizhou by Wignall et al. (2009) in magnitude. The very sharp negative shift at these three sections suggests that the two topmost Capitanian conodont zones at Penglaitan (*Jinogondolella granti* Zone and *Clarkina postbitteri hongshuiensis* Subzone) are missing if the negative excursions are correlative with that reported by Wignall et al. (2009).

This is an author-produced, peer-reviewed version of this article. The final, definitive version of this document can be found online at *Earth and Planetary Science Letters*, published by Elsevier. Copyright restrictions may apply. DOI: 10.1016/j.epsl.2013.05.020.

The absence of the GLB excursion at the Kuh-e-Alibashi section in NW Iran and the near constant value of +4‰ in the lower part of the section is interpreted to indicate that the base of the section is higher than the GLB. Our conodont biostratigraphic data (Shen and Mei, 2010) suggested that the lowest conodont zone at the Kuh-e-Alibashi section is advanced *Clarkina dukouensis* (Shen and Mei, 2010).

The large negative excursions in the Late Guadalupian reported by Wignall et al. (2009) in Guizhou, south China and this study are not present at the Shahreza (Korte and Kozur, 2010; Korte et al., 2004b) and the Abadeh section in central Iran (Liu et al., 2013). C-isotope profiles from Unit 5 in Shahreza and Abadeh indicate no large negative excursions, but a relatively minor negative excursion about 2‰ with frequent fluctuation is present in the uppermost part of Unit 5 in Abadeh, which marks the GLB in Iran (Liu et al., 2013) (Fig. 3).

The Wuchiapingian-Changhsingian boundary excursions

$\delta^{13}C$ depletion with various patterns across the WCB has been detected from all four sections in South China (Fig. 2). The C-isotope values are significantly more positive, mostly around +4‰ from the lower part of the Lopingian above the GLB. This Wuchiapingian positive plateau is followed by two negative shifts between 3.5-6.5‰ separated by a short positive excursion between 2-4‰ in south China. The lower negative shift spans a part of the *Clarkina liangshanensis* and *C. orientalis* conodont zones; the intervening positive excursion is approximately around the WCB and the upper negative shift is in the basal part of the Changhsingian. Recovery to stable values occurred in the early Changhsingian *C. subcarinata* Zone in all four investigated sections in south China (Fig. 2).

The negative excursions are not completely expressed in the basal part of the Meishan section. The minor positive peak at the WCB, the upper negative shift and the rapid recovery in the basal part of the Changhsingian are generally comparable with the other sections. Some very negative values of $\delta^{13}C_{carb}$ and large fluctuations are detected from the core samples in the upper part of the Lungtan Formation, which is difficult to interpret. One potential explanation for those anomalous negative values is that the incorporation of ^{12}C derived from oxidized organic matter from the organic-rich sediments with low $CaCO_3$ in the upper part of the Lungtan Formation. However, the magnitude of the negative excursions around the WCB at the Meishan section may truly reflect seawater values or more likely the combined influence of primary signals, diagenesis and facies change. An analysis for carbon and oxygen isotope values from the Meishan section shows no correlation between them and nearly all the oxygen values are between -5‰ and -9‰, thus, obvious diagenesis is not supported by the data (data repository).

A large broad negative shift of 6.3‰ and a minor negative shift of 3‰ around the WCB occur at the Shangsi section. The first negative shift is much larger in magnitude than all other sections documented herein. Oxygen isotope values within this excursion are all between -3‰ and -8‰ and no correlation is present between $\delta^{13}C$ and $\delta^{18}O$ profiles (data repository). Both $\delta^{13}C_{carb}$ and $\delta^{13}C_{org}$ profiles from a part of the Lopingian of the Shangsi section were reported by Bai et al. (2008). A general depletion of about 6‰ within a 20-m interval in the middle part of the Talung Formation at the Shangsi section was reported. However, the positive rebound to +1.5‰ at the WCB between two negative excursions was not detected. Both organic and inorganic carbon isotopes for the Changhsingian and Lower Triassic were analyzed by Riccardi et al. (2007) from the Shangsi section. The

This is an author-produced, peer-reviewed version of this article. The final, definitive version of this document can be found online at *Earth and Planetary Science Letters*, published by Elsevier. Copyright restrictions may apply. DOI: 10.1016/j.epsl.2013.05.020.

$\delta^{13}C_{carb}$ profile they published is characterized by a distinct negative shift near the WCB followed by a steady increase in the early Changhsingian and a sharp negative shift at the end-Permian that are comparable with our results, but they sampled at lower resolution and did not sample the Wuchiaping Formation. Therefore, the $\delta^{13}C_{carb}$ fluctuations we report in the late Wuchiapingian were not captured in their study.

The C-isotope profile from the Dukou section shows a different pattern from the above sections. A very broad depletion of about 3‰ begins in the *Clarkina guangyuanensis* Zone and spans the whole *C. orientalis* Zone, which indicates that the *C. orientalis* Zone at the Dukou section is highly expanded (Fig. 2). This interpretation is supported by a previous conodont studies from this section (Mei et al., 1994b) as well as our own data.

The Late Permian $\delta^{13}C_{carb}$ profile from Kuh-e-Alibashi in NW Iran is generally comparable with those documented from south China. A negative shift begins in the uppermost part of the *Clarkina liangshanensis* Zone and spans the whole *C. orientalis* Zone to the *C. subcarinata* Zone, but its upper negative excursion is poorly displayed by the data based on relatively coarse sampling. The double negative pattern is neither detected from Shahreza by Korte et al. (2004b) and Korte and Kozur (2010) nor Abadeh (Richoz, 2006) in central Iran. A negative excursion with a magnitude of 0.9-1.5‰ at about 15 m below the PTB at the Abadeh section was reported by Richoz et al. (2010), but they sampled the lower part of the section sparsely. This $\delta^{13}C_{carb}$ excursion has been confirmed recently by Liu et al. (2013) based on high-resolution samples correlated to the WCB based on strontium isotope chemostratigraphy at the Abadeh section (Fig. 3). This pattern is comparable to that at the Dukou section, but the pattern with two negative excursions in other south China sections is not comparable. The magnitude is much smaller and the early Changhsingian recovery is more gradual in terms of the section thickness (Liu et al., 2013). This negative excursion was placed in the *Clarkina* “*leveni*” Zone by Richoz et al. (2010), but conodonts from central Iran need additional study with sample population approach (Shen and Mei, 2010). The Lopingian $\delta^{13}C_{carb}$ profile in central Iran has been well documented from another section at Shahreza. The general pattern is basically comparable with that at Abadeh. However, the depletion is minimal and not obvious (Fig. 3).

Secular changes of Lopingian $\delta^{13}C_{carb}$have also been documented from the Gartnerkofel core in Austria (Magaritz et al., 1992). The $\delta^{13}C_{carb}$ curve shows a gradual increase in Unit 1A of the Bellerophon Formation, which may be correlative with the upper part of the WCB excursions, but without good biostratigraphic constraints. Similar $\delta^{13}C_{carb}$ curves spanning the WCB have been also reported from Wadi Sahtan, Çürük Dağ (Richoz, 2006), the Buday’ah sectionin Oman (Baud et al., 2012) and the Salt Range, Pakistan (Baud et al., 1996), but no distinct negative shift around the WCB have been detected. The failure to capture the negative shift at the WCB in those sections may reflect insufficient sample resolution or the WCB excursion is only reflected at a regional scale.

Overall, the negative excursion around the WCB shows different magnitudes and patterns. It began in the middle Wuchiapingian *Clarkina liangshanensis* Zone and ended in the early Changhsingian *C. subcarinata* Zone. According to the dates of the ash beds in the Wuchiaping and Talung formations at the Shangsi section, this negative excursion began at about 258 Ma, about 5.8 Myr prior to the end-Permian extinction, and ended 4.5 Myr later at about 253.5 Ma (Shen et al., 2011) (Fig. 2). The Changhsingian shows a positive excursion to values around +2-4‰ from the upper part of the conodont *C. subcarinata* Zone to the *C. yini* Zone, which is followed by the end-Changhsingian major negative excursion.

This is an author-produced, peer-reviewed version of this article. The final, definitive version of this document can be found online at *Earth and Planetary Science Letters*, published by Elsevier. Copyright restrictions may apply. DOI: 10.1016/j.epsl.2013.05.020.

The end-Changhsingian negative excursion

The large, sharp carbon isotope depletion of about 5-6‰ slightly prior to the PTB, which is associated with the end-Permian mass extinction, has been extensively documented (see a review by Korte and Kozur, 2010). This excursion is characterized by a decline of 2‰ in $\delta^{13}C$ over 90,000 years beginning from ~252.4 Ma, and followed by a $\delta^{13}C$ excursion of 5‰ that is at the top of Bed 24e at the Meishan section (Cao et al., 2009). Biostratigraphically, the gradual decline began at the base of the *Clarkina yini* Zone at the Meishan section and the sharp 5‰ negative excursion occurred within the *C. meishanensis* Zone. The negative shift in the latest Changhsingian is very short in terms of the rock thickness, which indicates the PTB interval is highly condensed or some short hiatuses are possibly present around the PTB at the Meishan and Shangsi sections (e.g., Hermann et al., 2010) (Fig. 2). The same negative excursion is represented by a much thicker interval at the Matan section with relatively higher sediment accumulation rate, but also began slightly below the tuffaceous bed of 252.41±0.08 Ma and in the *C. yini* Zone. Recently, Luo et al. (2011) recognized a stepwise pattern of the end-Changhsingian carbon isotope excursion, with the shift preceding the end-Permian mass extinction larger than that following it. The pattern documented by Luo et al. (2011) is temporally identical with our excursion, but not consistent with our patterns shown here, which suggest that the negative shift in the extinction interval is much larger and more rapid than that preceding it. It is highly likely that the different patterns reported from south China are due to variation in sediment accumulation rates near the extinction interval because of frequent sea-level changes and intensive soil erosion associated with the terrestrial extinction in south China (Shen et al., 2011).

The large negative excursion around the PTB is clearly expressed in Iran. All four sections show an identical pattern, which corresponds well with that in south China (Fig. 3), except that the biostratigraphic placement differs based on the conodont zones for Iran reported by Kozur (2004; 2005). According to Kozur (2004; 2005), the gradual depletion began in the conodont *Clarkina bachmanni* Zone, below the *C. changxingensis-C. deflecta* Zone and above the *C. subcarinata* Zone. If this conodont zonation is followed, then the gradual depletion began in the early Changhsingian based on the same conodont zonation at Meishan, south China, which conflicts with all PTB $\delta^{13}C$ patterns documented worldwide. However, the conodonts from Kuh-e-Alibashi and Zal in NW Iran and Abadeh in central Iran have been restudied by Shen and Mei (2010) and Henderson et al. (2008). According to Shen and Mei (2010, fig. 13), the *C. bachmanni*, *C. nodosa* and *C. jolfensis* zones in Iran are all together largely equivalent to the *C. yini* Zone in south China. Based on this correlation, the gradual $\delta^{13}C$ depletion started in the base of *C. yini* Zone, which is consistent with the $\delta^{13}C$ pattern in time at the Meishan section (Fig. 3).

A COMPOSITE $\delta^{13}C_{carb}$ CHEMOSTRATIGRAPHIC FRAMEWORK FOR THE LOPINGIAN

The chemostratigraphic data presented here for south China and Iran establish a new composite $\delta^{13}C$ profile for Lopingian marine carbonates (Fig. 4). This composite $\delta^{13}C$ profile consists of the most high-resolution data from both south China and Iran, which can be used as a correlation tool and a proxy of the state of carbon cycle prior to the end-Permian mass extinction. It is particularly important to understand the tempo of the end-Permian mass extinction within high-resolution biostratigraphic framework constrained by high-precision geochronology. As shown in Figures 2-4, distinct negative excursions occurred from the latest Guadalupian to the end-Changhsingian.

This is an author-produced, peer-reviewed version of this article. The final, definitive version of this document can be found online at *Earth and Planetary Science Letters*, published by Elsevier. Copyright restrictions may apply. DOI: 10.1016/j.epsl.2013.05.020.

The large negative excursion just before the GLB is followed by a rapid positive shift of 4-6‰ until the latest Guadalupian, which is followed by a minor negative shift at the GLB, then immediately recovered in the *Clarkina dukouensis* Zone. $\delta^{13}C$ values show a gradual decline from the *C. dukouensis* to the *C. guangyuanensis* (or *C. transcaucasica* or lower part of *C. liangshanensis* Zone) (Fig. 4). This gradual decline lasted about 1.5 Myr based on a GLB age estimate of 259.8 Ma (Henderson et al., 2012). It is followed by a minor recovery. Then, another relatively long negative excursion of 2.6-6.3‰ occurred from the *C. liangshanensis* Zone to the lower part of the *C. orientalis* Zone (Figs. 2, 4). This prolonged negative excursion is not fully revealed in the Meishan core samples because carbonate strata are not available. It is represented by more than 120m at the Dukou section with a more gentle depletion (*ca.* 2.8‰). The long-term negative excursion is interrupted by a minor positive recovery below the WCB in Matan and Shangsi sections, but not well expressed in the Dukou section. According to the most recent dates from ash beds in the three sections, this long-term negative excursion began about 5.8Myr prior to the end-Permian mass extinction. The WCB is characterized by another distinct negative shift between 2-4‰, but is highly variable in magnitude among sections and does not occurin Iran (Figs. 2, 3). For most of the Changhsingian, from the upper part of the conodont *Clarkina subcarinata* Zone to the *C. yini* Zone, the $\delta^{13}C_{carb}$values remained between +2-4‰ (Figs. 2, 4). This interval of stability wasfollowed by the rapid depletion associated with the end-Permian mass extinction (Cao et al., 2009; Shen et al., 2011).

The Lopingian composite $\delta^{13}C$ profile presented here still needs to be refined as new isotopic data are produced and the biostratigraphic, taxonomic and geochronologic data are improved. In Figure 4, we show a $\delta^{13}C$ profile scaled to radioisotopic dates from the Shangsi section. Several temporal ambiguities of $\delta^{13}C$ excursions are worth noting. First, a negative excursion in $\delta^{13}C$ began in the *Jinogondolella xuanhanensis* Zone of latest Capitanian age. This Late Capitanian negative excursion also occurs at the Dukou, Shangsi and Heshan sections, but has not yet been recovered at Penglaitan and Tieqiao (Chen et al., 2011). The negative excursion at the GLB at Penglaitan and Tieqiao reported by Wang et al. (2004) and at Kamura in Japan by Isozaki et al. (2007) is not the same excursion documented by Wignall et al. (2009), which is 2-3 conodont zones below, and much larger (Fig. 4). Second, the paired negative excursions around the WCB began in the *Clarkina liangshanensis* Zone and ended just above the WCB in the *C. subcarinata* Zone with highly variable magnitude and overall pattern. Third, the $\delta^{13}C$ profiles at the end of the Changhsingian in Iran can be precisely correlative with that at the Meishan section (Figs. 3, 4).

DISCUSSION

The bulk carbon isotope records for the entire Lopingian of south China and Iran suggest that major global carbon cycle perturbations could occur during Late Permian, prior to the end-Permian mass extinction. However, variability in the pattern of isotope variation across sections leaves the possibility open that some of these excursions reflect local or regional controls rather than global disturbances of carbon cycling. Our data show that a large negative carbon isotope excursion occurred from the topmost part of the conodont *Jinogondolella xuanhanensis* Zone and recovered around GLB. This excursion coincides with the eruption of the Emeishan basalts in south China, which have been widely interpreted as the cause of the end-Guadalupian crisis (Wignall et al., 2009; Zhong et al., 2013; Zhou et al., 2002). However, spatial variation in magnitude of the excursion is evident in our data. The negative excursion is relatively weakly displayed at the Shangsi section with the shallow water carbonate facies, but very strongly reflected at the Dukou section with the relatively deep-water cherty carbonate.

This is an author-produced, peer-reviewed version of this article. The final, definitive version of this document can be found online at *Earth and Planetary Science Letters*, published by Elsevier. Copyright restrictions may apply. DOI: 10.1016/j.epsl.2013.05.020.

The temporal overlap between the Emeishan volcanism and the negative carbon isotope excursion below the GLB is incompatible with recent radioisotopic dates on Emeishan volcanics (Shellnutt et al., 2012). According to Shellnutt et al. (2012), Emeishan volcanism began during late Capitanian time and ended by 257 Ma, which is in the middle Wuchiapingian; thus, the Emeishan volcanism had much longer duration although it overlapped with negative carbon excursion. New radioisotopic dates from the Karoo Basin of South Africa indicates that the previously reported end-Guadalupian terrestrial mass extinction is not consistent with the GLB (Rubidge et al., 2013). Eruption of the Emeishan basalts began during the Late Guadalupian, as indicated by volcanic ashes genetically related to the Emeishan large igneous province in the Late Guadalupian *Jinogondolella granti* Zone at the Penglaitan GSSP section (Zhong et al., 2013), but exact time of onset of the Emeishan volcanism and whether it is related to the GLB carbon excursion is unclear.

The negative excursions around the WCB (Fig. 4) display complex spatial and temporal heterogeneity. At the Dukou section, which exhibits normal carbonate facies containing abundant fusulinids and brachiopods, the negative excursion in $\delta^{13}C_{carb}$ is only 2.8‰. At the Matan section, which is characterized by a coal-bearing sequence that formed in a shallow water carbonate platform facies interbedded with nearshore peat flat facies and coastal lagoon facies, the negative excursion is 5.3‰. In the Shangsi section, characterized by deep-water facies, the carbon isotope values shift by 6.3‰. In the Dzhulfian part of the Abadeh and Shahreza sections, the magnitude of this negative excursion is only 1.3‰. The Kuh-e-Alibashi section in Iran, which exhibits similar facies to the Abadeh and Shahreza sections, shows an excursion of about 3.9‰. Thus, both the magnitude of the shift and the most negative values of the late Wuchiapingian negative shift are more profound in deep-water facies than in shallow-water facies, but there is not a definite correlation with water depth based on the sections of south China. This spatial heterogeneity is unlike the $\delta^{13}C_{carb}$ excursions just below the PTB, which exhibit similar magnitudes and most negative values regardless of lithofacies or depositional setting (Figs. 2, 3). Thus, the differences in magnitude among sections likely reflect local, depth-related factors such as the supply of organic matter to the sediment, isotope gradients within the water column, or facies controls on diagenesis (Saltzman and Thomas, 2012). There may also be a connection between sea level change and the $\delta^{13}C_{carb}$ of sediments in marginal settings (Swart, 2008). Thus, it is not clear whether the GLB and WCB negative excursions are related to the changes of global carbon cycle. It is evident that the GLB excursion occurred during eruption of the Emeishan flood basalts and coincided with the loss of some benthic fossils (e.g., fusulinds and rugose corals), but no similar links to geological or biological events are currently known for the WCB excursion (Fig. 4).

Both the GLB and WCB carbon isotope excursions were not associated with distinct biodiversity changes in terms of taxon richness (Fig. 4). The intensity of the end-Guadalupian extinction is little different from Permian background rates for benthic marine invertebrates (Clapham et al., 2009) and there was no associated terrestrial extinction event (Rubidge et al., 2013). Similarly, the ecological impact of this event was minor in the sense of Droser et al. (2000). However, differences in selectivity patterns relative to other background stages (Clapham and Payne, 2011) as well as more severe taxonomic losses in a few clades, such as fusulinids and rugose corals (Groves and Yue, 2009; Wang and Sugiyama, 2000), point toward a global environmental perturbation, albeit of much smaller magnitude than the end-Changhsingian event. The relatively low diversity in the early Wuchiapingian is most likely due to a species-area effect since very few marine deposits with abundant fossils

This is an author-produced, peer-reviewed version of this article. The final, definitive version of this document can be found online at *Earth and Planetary Science Letters*, published by Elsevier. Copyright restrictions may apply. DOI: 10.1016/j.epsl.2013.05.020.

are available in the world because of the global end-Guadalupian regression. However, once early Wuchiapingian transgressive marine deposits become available, high-diversity benthic faunas occur (e.g., Fang, 1987; Shen and Zhang, 2008); most fossil groups did not suffered a catastrophic loss during the end-Guadalupian extinction.

Unlike the GLB and WCB excursions, the $\delta^{13}C_{carb}$ excursion across the PTB in all eight sections in south China and Iran reveals a consistent rapid *ca.* 5‰ negative shift associated with the mass extinction (Fig. 4). This negative shift is preceded by a positive plateau through most of the Changhsingian with $\delta^{13}C_{carb}$ values about +2-4‰. This pattern indicates that the $\delta^{13}C_{carb}$ negative excursion just below the PTB is not dependent upon facies change, therefore, reflects global changes in carbon cycle.

The end-Guadalupian and end-Changhsingian negative carbon isotope excursions are temporally consistent with frequent volcanic eruptions in south China and Siberia (Bowring et al., 1998; Mundil et al., 2004; Renne et al., 1995; Shen et al., 2011; Wignall et al., 2009; Zhou et al., 2002) (Fig. 4). Both may have been caused by volcanic outgassing. However, C-cycle modeling (e.g., Berner, 2002; Shen et al., 2011) suggests that introduction of carbon with the isotope composition of volcanic (i.e., mantle) CO_2 produces only smaller negative carbon isotope excursions followed by larger and more protracted positive excursions, which is insufficient to explain the magnitudes of the PTB or GLB $\delta^{13}C$ excursions. Another possibility is that intense volcanism or dike swarms into the continental margins may trigger rapid massive release of methane from the dissociation of marine gas hydrates and carbon from thick organic-rich deposits (Heydari et al., 2008; Saunders and Reichow, 2009; Svensen et al., 2009) or rapid venting of coal-derived methane or combustion of coal on continental and transitional deposits (Darcy and Norman, 2012; Grasby et al., 2011). The bulk of the methane would have been oxidized aerobically in the water column to produce CO_2 with low $\delta^{13}C$ values, which is sufficient to explain a $\delta^{13}C$ shift of 7-8‰ (Berner, 2002; Regnier et al., 2011). However, this scenario is not applicable for the WCB excursions. The high variability of the WCB carbon isotope excursions lasted more than 4 Myr which are incompatible with methane release from seafloor gas hydrates because insufficient time would be available between events for regenerating methan eclathrate reservoirs similar to the Early Triassic (cf. Payne et al., 2004). Increasing continental weathering by sea-level drop could have contributed to the lowering of $\delta^{13}C$ value, which has been documented at the end-Changhsingian and end-Guadalupian based on Late Permian sequence stratigraphy and petrologic studies. However, it conflicts with the perturbation around the WCB where there is no record of regression. Instead, a distinct regional transgression in the latest Wuchiapingian has been documented in south China (Li and Shen, 2008; Wang and Jin, 2000).

In summary, our results show that while carbon isotope excursions occur near the GLB, WCB, and PTB, the PTB excursion was by far the largest, the most consistently expressed in sections from different depositional environments, and the only one associated with catastrophic loss of biodiversity.

This is an author-produced, peer-reviewed version of this article. The final, definitive version of this document can be found online at *Earth and Planetary Science Letters*, published by Elsevier. Copyright restrictions may apply. DOI: 10.1016/j.epsl.2013.05.020.

References

Bai, X., Luo, G.M., Wu, X., Wang, Y.Z., Huang, J.H., and Wang, X.J., 2008, Carbon isotope records indicative of paleoceanographical events at the Latest Permian Dalong Formation at Shangsi, Northeast Sichuan, China: Journal of China University of Geosciences, v. 19, p. 481-487.

Baud, A., Atudorei, V., and Sharp, Z., 1996, Late Permian and early Triassic evolution of the Northern Indian margin: Carbon isotope and sequence stratigraphy: Geodinamica Acta, v. 9, p. 57-77.

Baud, A., Richoz, S., Beauchamp, B., Cordey, F., Grasby, S., Henderson, C.M., Krystyn, L., and Nicora, A., 2012, The Buday'ah Formation, Sultanate of Oman: A Middle Permian to Early Triassic oceanic record of the Neotethys and the late Induan microsphere bloom: Journal of Asian Earth Sciences, v. 43, p. 130-144.

Berner, R.A., 2002, Examination of hypotheses for the Permo-Triassic boundary extinction by carbon cycle modeling: Proceedings of the National Academy of Sciences of the United States of America, v. 99, p. 4172-4177.

Bowring, S.A., Erwin, D.H., Jin, Y.G., Martin, M.W., Davidek, K., and Wang, W., 1998, U/Pb zircon geochronology and tempo of the end-Permian mass extinction: Science, v. 280, p. 1039-1045.

Cao, C.Q., Love, G.D., Hays, L.E., Wang, W., Shen, S.Z., and Summons, R.E., 2009, Biogeochemical evidence for euxinic oceans and ecological disturbance presaging the end-Permian mass extinction event: Earth and Planetary Science Letters, v. 281, p. 188-201.

Chen, B., Joachimski, M.M., Sun, Y.D., Shen, S.Z., and Lai, X.L., 2011, Carbon and conodont apatite oxygen isotope records of Guadalupian–Lopingian boundary sections: Climatic or sea-level signal?: Palaeogeography, Palaeoclimatology, Palaeoecology, v. 311, p. 145-153.

Clapham, M.E., and Payne, J.L., 2011, Acidification, anoxia, and extinction: A multiple logistic regression analysis of extinction selectivity during the Middle and Late Permian: Geology, v. 39, p. 1059-1062.

Clapham, M.E., Shen, S.Z., and Bottjer, D.J., 2009, The double mass extinction revisited: reassessing the severity, selectivity, and causes of the end-Guadalupian biotic crisis (Late Permian): Paleobiology, v. 35, p. 32-50.

Darcy, E.O., and Norman, H.S., 2012, Explosive eruption of coal and basalt and the end-Permian mass extinction: Proceedings of the National Academy of Sciences, v. 109, p. 59-62.

Droser, M.L., Bottjer, D.J., Sheehan, P.M., and McGhee, G.R., 2000, Decoupling of taxonomic and ecologic severity of Phanerozoic marine mass extinctions: Geology, v. 28, p. 675-678.

Fang, Z.J., 1987, Bivalves from upper part of Permian in southern Hunan, China, *in* Palaeontology, N.I.o.G.a., ed., Nanjing Institute of Geology and Palaeontology, Academia Sinica, Collection of postgraduate theses: Nanjing, JIangsu Science and Technology Publishing House, p. 349-411, pls. 1-8.

Grasby, S.E., Sanei, H., and Beauchamp, B., 2011, Catastrophic dispersion of coal fly ash into oceans during the latest Permian extinction: Nature Geoscience, v. 4, p. 104-107.

Groves, J.R., and Yue, W., 2009, Foraminiferal diversification during the late Paleozoic ice age: Paleobiology, v. 35, p. 367-392.

Henderson, C.M., Davydov, V.I., and Wardlaw, B.R., 2012, The Permian Period, *in* Gradstein, F.M., Ogg, J.G., Schmitz, M.D., and Ogg, G.M., eds., The Geological time scale 2012, Volume vol. 2: Amsterdam, Elsevier, p. 653-680.

Henderson, C.M., Mei, S.L., Shen, S.Z., and Wardlaw, B.R., 2008, Resolution of the reported Upper Permian conodont occurrences from northwestern Iran: Permophiles p. 2-9.

This is an author-produced, peer-reviewed version of this article. The final, definitive version of this document can be found online at *Earth and Planetary Science Letters*, published by Elsevier. Copyright restrictions may apply. DOI: 10.1016/j.epsl.2013.05.020.

Hermann, E., Hochuli, P.A., Bucher, H., Vigran, J.O., Weissert, H., and Bernasconi, S.M., 2010, A close-up view of the Permian–Triassic boundary based on expanded organic carbon isotope records from Norway (Trøndelag and Finnmark Platform): Global and Planetary Change, v. 74, p. 156-167.

Heydari, E., Arzani, N., and Hassanzadeh, J., 2008, Mantle plume: The invisible serial killer -- Application to the Permian-Triassic boundary mass extinction: Palaeogeography, Palaeoclimatology, Palaeoecology, v. 264, p. 147-162.

Horacek, M., Brandner, R., and Abart, R., 2007, Carbon isotope record of the P/T boundary and the Lower Triassic in the Southern Alps: Evidence for rapid changes in storage of organic carbon: Palaeogeography, Palaeoclimatology, Palaeoecology, v. 252, p. 347-354.

Isozaki, Y., Kawahata, H., and Ota, A., 2007, A unique carbon isotope record across the Guadalupian–Lopingian (Middle–Upper Permian) boundary in mid-oceanic paleo-atoll carbonates: The high-productivity "Kamura event" and its collapse in Panthalassa: Global and Planetary Change, v. 55, p. 21-38.

Jin, Y.G., Shen, S.Z., Henderson, C.M., Wang, X.D., Wang, W., Wang, Y., Cao, C.Q., and Shang, Q.H., 2006, The Global Stratotype Section and Point (GSSP) for the boundary between the Capitanian and Wuchiapingian stage (Permian): Episodes, v. 29, p. 253-262.

Kaiho, K., Chen, Z.Q., Ohashi, T., Arinobu, T., Sawada, K., and Cramer, B.S., 2005, A negative carbon isotope anomaly associated with the earliest Lopingian (Late Permian) mass extinction: Palaeogeography Palaeoclimatology Palaeoecology, v. 223, p. 172-180.

Korte, C., and Kozur, H.W., 2010, Carbon-isotope stratigraphy across the Permian-Triassic boundary: A review: Journal of Asian Earth Sciences, v. 39, p. 215-235.

Korte, C., Kozur, H.W., Joachimski, M.M., Strauss, H., Veizer, J., and Schwark, L., 2004a, Carbon, sulfur, oxygen and strontium isotope records, organic geochemistry and biostratigraphy across the Permian/Triassic boundary in Abadeh, Iran: International Journal of Earth Sciences, v. 93, p. 565-581.

Korte, C., Kozur, H.W., and Mohtat-Aghai, P., 2004b, Dzhulfian to lowermost Triassic $d^{13}C$ record at the Permian/Triassic boundary section at Shahreza, Central Iran, Reihe B: Hallesches Jahrb. Geowiss, v. Beiheft 18, p. 73-78.

Kozur, H.W., 2004, Pelagic uppermost Permian and the Permian-Triassic boundary conodonts of Iran. Part 1: taxonomy: Hallesches Jahrbuch Für Geowissenschaften, Reihe B: Geologie, Paläontologie, Mineralogie, v. 18, p. 39-68.

Kozur, H.W., 2005, Pelagic uppermost Permian and the Permian-Triassic boundary conodonts of Iran, Part II: Investigated sections and evaluation of the conodont faunas: Hallesches Jahrbuch Für Geowissenschaften, Reihe B: Geologie, Paläontologie, Mineralogie, v. 19, p. 49-86.

Li, W.Z., and Shen, S.Z., 2008, Lopingian (Late Permian) brachiopods around the Wuchiapingian-Changhsingian boundary at the Meishan Sections C and D, Changxing, South China: Geobios, v. 41, p. 307-320.

Li, Z.S., Zhan, L.P., Dai, J.Y., Jin, R.G., Zhu, X.F., Zhang, J.H., Huang, H.Q., Xu, D.Y., Yan, Z., and Li, H.M., 1989, Study on the Permian-Triassic biostratigraphy and event stratigraphy of northern Sichuan and southern Shaanxi: Beijing, Geological Publishing House, 435 p.

Liu, X.C., Wang, W., Shen, S.Z., Gorgij, M.N., Ye, F.C., Zhang, Y.C., Furuyama, S., Kano, A., and Chen, X.Z., 2013, Late Guadalupian to Lopingian (Permian) carbon and strontium isotopic chemostratigraphy in the Abadeh section, central Iran: Gondwana Research.

Luo, G.M., Wang, Y.B., Yang, H., Algeo, T.J., Kump, L.R., Huang, J.H., and Xie, S.C., 2011, Stepwise and large-magnitude negative shift in $d^{13}C_{carb}$ preceded the main marine mass extinction of the Permian-Triassic crisis interval: Palaeogeography, Palaeoclimatology, Palaeoecology, v. 299, p. 70-82.

This is an author-produced, peer-reviewed version of this article. The final, definitive version of this document can be found online at *Earth and Planetary Science Letters*, published by Elsevier. Copyright restrictions may apply. DOI: 10.1016/j.epsl.2013.05.020.

Magaritz, M., Krishnamurthy, R.V., and Holser, W.T., 1992, Parallel trends in organic and inorganic carbon isotopes across the Permian Triassic boundary: American Journal of Science, v. 292, p. 727-739.

Mei, S.L., Henderson, C.M., and Cao, C.Q., 2004, Conodont sample-population approach to defining the base of the Changhsingian Stage, Lopingian Series, Upper Permian. The palynology and micropalaeontology of boundaries: Geological Society Special Publications, v. 230, p. 105-121.

Mei, S.L., Jin, Y.G., and Wardlaw, B.R., 1994a, Succession of conodont zones from the Permian “Kuhfeng” Formation, Xuanhan, Sichuan and its implications in global correlation: Acta Palaeontologica Sinica, v. 33, p. 1-23.

Mei, S.L., Jin, Y.G., and Wardlaw, B.R., 1994b, Sucession of Wuchiapingian conodonts from northeastern Sichuan and its worldwide correlation: Acta Micropalaeontologica Sinica, v. 11, p. 121-139.

Mundil, R., Ludwig, K.R., Metcalfe, I., and Renne, P.R., 2004, Age and timing of the Permian mass extinctions: U/Pb dating of closed-system zircons: Science, v. 305, p. 1760-1763.

Payne, J.L., Lehrmann, D.J., Wei, J., Orchard, M.J., Schrag, D.P., and Knoll, A.H., 2004, Large perturbations of the carbon cycle during recovery from the end-permian extinction: Science, v. 305, p. 506-509.

Regnier, P., Dale, A.W., Arndt, S., LaRowe, D.E., Mogollón, J., and Van Cappellen, P., 2011, Quantitative analysis of anaerobic oxidation of methane (AOM) in marine sediments: A modeling perspective: Earth-Science Reviews, v. 106, p. 105-130.

Renne, P.R., Zhang, Z.C., Richards, M.A., Black, M.T., and Basu, A.R., 1995, Synchrony and causal relations between Permian-Triassic boundary crises and Siberian flood volcanism: Science, v. 269, p. 1413-1416.

Retallack, G.J., and Jahren, A.H., 2008, Methane release from igneous intrusion of coal during Late Permian extinction events: Journal of Geology, v. 116, p. 1-20.

Riccardi, A., Kump, L.R., Arthur, M.A., and D'Hondt, S., 2007, Carbon isotopic evidence for chemocline upward excursions during the end-Permian event: Palaeogeography, Palaeoclimatology, Palaeoecology, v. 248, p. 73-81.

Richoz, S., 2006, Stratigraphie et variations isotopiques du carbone dans le Permien supérieur et le Trias inférieur de quelques localités de la Néotéthys (Turquie, Oman et Iran): Mémoire de Géologie de Lausanne, v. 46, p. 1-275.

Richoz, S., Krystyn, L., Baud, A., Brandner, R., Horacek, M., and Mohtat-Aghai, P., 2010, Permian-Triassic boundary interval in the Middle East (Iran and N. Oman): Progressive environmental change from detailed carbonate carbon isotope marine curve and sedimentary evolution: Journal of Asian Earth Sciences, v. 39, p. 236-253.

Rubidge, B.S., Erwin, D.H., Ramezani, J., Bowring, S.A., and de Klerk, W.J., 2013, High-precision temporal calibration of Late Permian vertebrate biostratigraphy: U-Pb zircon constraints from the Karoo Supergroup, South Africa: Geology, v. 41, p. 363-366.

Saltzman, M.R., and Thomas, E., 2012, Carbon isotope stratigraphy, *in* Gradstein, F.M., Ogg, J.G., Schmitz, M.D., and Ogg, G.M., eds., The Geologic Time Scale 2012, Volume 1: Amsterdam, Elsevier, p. 207-232.

Saunders, A., and Reichow, M., 2009, The Siberian Traps and the End-Permian mass extinction: a critical review: Chinese Science Bulletin, v. 54, p. 20-37.

Shao, L.Y., Zhang, P.F., Gayer, R.A., Chen, J.L., and Dai, S.F., 2003, Coal in a carbonate stratigraphic framework: the Upper Permian Heshan Formation in central Guangxi, southern China: Journal of Geological Society of London v. 160, p. 285-298.

Shellnutt, J.G., Denyszyn, S.W., and Mundil, R., 2012, Precise age determination of mafic and felsic intrusive rocks from the Permian Emeishan large igneous province (SW China): Gondwana Research, v. 22, p. 118-126.

This is an author-produced, peer-reviewed version of this article. The final, definitive version of this document can be found online at *Earth and Planetary Science Letters*, published by Elsevier. Copyright restrictions may apply. DOI: 10.1016/j.epsl.2013.05.020.

Shen, J., Algeo, T.J., Hu, Q., Zhang, N., Zhou, L., Xia, W., Xie, S., and Feng, Q., 2012, Negative C-isotope excursions at the Permian-Triassic boundary linked to volcanism: Geology, v. 40, p. 963-966.

Shen, S.Z., Crowley, J.L., Wang, Y., Bowring, S.A., Erwin, D.H., Sadler, P.M., Cao, C.Q., Rothman, D.H., Henderson, C.M., Ramezani, J., Zhang, H., Shen, Y., Wang, X.D., Wang, W., Mu, L., Li, W.Z., Tang, Y.G., Liu, X.L., Liu, L.J., Zeng, Y., Jiang, Y.F., and Jin, Y.G., 2011, Calibrating the end-Permian mass extinction: Science, v. 334, p. 1367-1372.

Shen, S.Z., Henderson, C.M., Bowring, S.A., Cao, C.Q., Wang, Y., Wang, W., Zhang, H., Zhang, Y.C., and Mu, L., 2010, High-resolution Lopingian (Late Permian) timescale of South China: Geological Journal, v. 45, p. 122-134.

Shen, S.Z., and Mei, S.L., 2010, Lopingian (Late Permian) high-resolution conodont biostratigraphy in Iran with comparison to South China zonation: Geological Journal, v. 45, p. 135-161.

Shen, S.Z., and Zhang, Y.C., 2008, Earliest Wuchiapingian (Lopingian, late Permian) brachiopods in southern Hunan, South China: implications for the pre-Lopingian crisis and onset of Lopingian recovery/radiation: Journal of Paleontology, v. 82, p. 924-937.

Svensen, H., Planke, S., Polozov, A.G., Schmidbauer, N., Corfu, F., Podladchikov, Y.Y., and Jamtveit, B., 2009, Siberian gas venting and the end-Permian environmental crisis: Earth and Planetary Science Letters, v. 277, p. 490-500.

Swart, P.K., 2008, Global synchronous changes in the carbon isotopic composition of carbonate sediments unrelated to changes in the global carbon cycle: Proceedings of the National Academy of Sciences of the United States of America, v. 105, p. 13741-13745.

Teichert, C., Kummel, B., and Sweet, W., 1973, Permian-Triassic strata, Kuh-e-Ali Bashi, northwestern Iran: Bulletin of the Museum of Comparative Zoology, v. 145, p. 359-472.

Tong, J., Zuo, J., and Chen, Z.Q., 2007, Early Triassic carbon isotope excursions from South China: Proxies for devastation and restoration of marine ecosystems following the end-Permian mass extinction: Geological Journal, v. 42, p. 371-389.

Wang, W., Cao, C.Q., and Wang, Y., 2004, The carbon isotope excursion on GSSP candidate section of Lopingian-Guadalupian boundary: Earth and Planetary Science Letters, v. 220, p. 57-67.

Wang, X.D., and Sugiyama, T., 2000, Diversity and extinction patterns of Permian coral faunas of China: Lethaia, v. 33, p. 285-294.

Wang, Y., and Jin, Y.G., 2000, Permian palaeogeographic evolution of the Jiangnan Basin, South China: Palaeogeography Palaeoclimatology Palaeoecology, v. 160, p. 35-44.

Wignall, P.B., Bond, D.P.G., Haas, J., Wang, W., Jiang, H.S., Lai, X.L., Altiner, D., Vedrine, S., Hips, K., Zajzon, N., Sun, Y.D., and Newton, R.J., 2012, Capitanian (Middle Permian) mass extinction and recovery in western Tethys: a fossil, facies, and $\delta^{13}C$ study from Hungary and Hydra island (Greece): Palaios, v. 27, p. 78-89.

Wignall, P.B., Sun, Y.D., Bond, D.P.G., Izon, G., Newton, R.J., Vedrine, S., Widdowson, M., Ali, J.R., Lai, X.L., Jiang, H.S., Cope, H., and Bottrell, S.H., 2009, Volcanism, mass extinction, and carbon isotope fluctuations in the Middle Permian of China: Science, v. 324, p. 1179-1182.

Zhong, Y.T., He, B., and Xu, Y.G., 2013, Mineralogy and geochemistry of claystones from the Guadalupian–Lopingian boundary at Penglaitan, South China: Insights into the pre-Lopingian geological events: Journal of Asian Earth Sciences, v. 62, p. 438-462.

Zhou, M.F., Malpas, J., Song, X.Y., Robinson, P.T., Sun, M., Kennedy, A.K., Lesher, C.M., and Keays, R.R., 2002, A temporal link between the Emeishan large igneous province (SW China) and the end-Guadalupian mass extinction: Earth and Planetary Science Letters, v. 196, p. 113-122.

This is an author-produced, peer-reviewed version of this article. The final, definitive version of this document can be found online at *Earth and Planetary Science Letters*, published by Elsevier. Copyright restrictions may apply. DOI: 10.1016/j.epsl.2013.05.020.

Fig. 1. Locality and reconstruction map showing the studied areas. A, south China; 1, Meishan; 2, Shangsi; 3, Dukou; 4, Matan in Heshan; base map after Wang and Jin (2000). B, Iran; 5, Kuh-e-Alibash section; 6, Zal section; 7, Shahreza section; 8, Abadeh section. C, Changhsingian reconstruction map showing the paleogeographic positions of the studied sections.

Fig. 2. Lopingian $\delta^{13}C_{carb}$ chemostratigraphy of south China. Conodont zones are established based on sample population approach of Mei et al. (2004) and Shen and Mei (2010). Data of the most part of Changhsing Formation and PTB interval at Meishan are from Cao et al. (2009). Geochronologic ages are from Shen et al. (2011).

Fig. 3. Lopingian $\delta^{13}C_{carb}$ chemostratigraphy of Iran. Conodont zones are combined from Shen and Mei (2010) for Kuh-e-Alibashi and Abadeh, Henderson et al. (2008) for Zal and Kozur (2004; 2005) for Shahreza. Carbon isotope data are from Korte et al. (2004b) (Shahreza); Richoz(2006) (Zal and Abadeh in purple) and Liu et al. (2013) (Abadeh in blue). Conodont biozones at Shahreza are from Kozur (2004).

Fig. 4. Lopingian (Late Permian) conodont biostratigraphy, 21-point moving average profile of $\delta^{13}C_{carb}$, volcanism and diversity pattern of south China. Scaled to the ages of the Shangsi section published by Shen et al. (2011). $\delta^{13}C_{carb}$ data included are from the Meishan, Heshan, Shangsi and Dukou sections. Diversity pattern in green reflects the pattern after removing the sampling effects (Shen et al., 2011).

This is an author-produced, peer-reviewed version of this article. The final, definitive version of this document can be found online at *Earth and Planetary Science Letters*, published by Elsevier. Copyright restrictions may apply. DOI: 10.1016/j.epsl.2013.05.020.

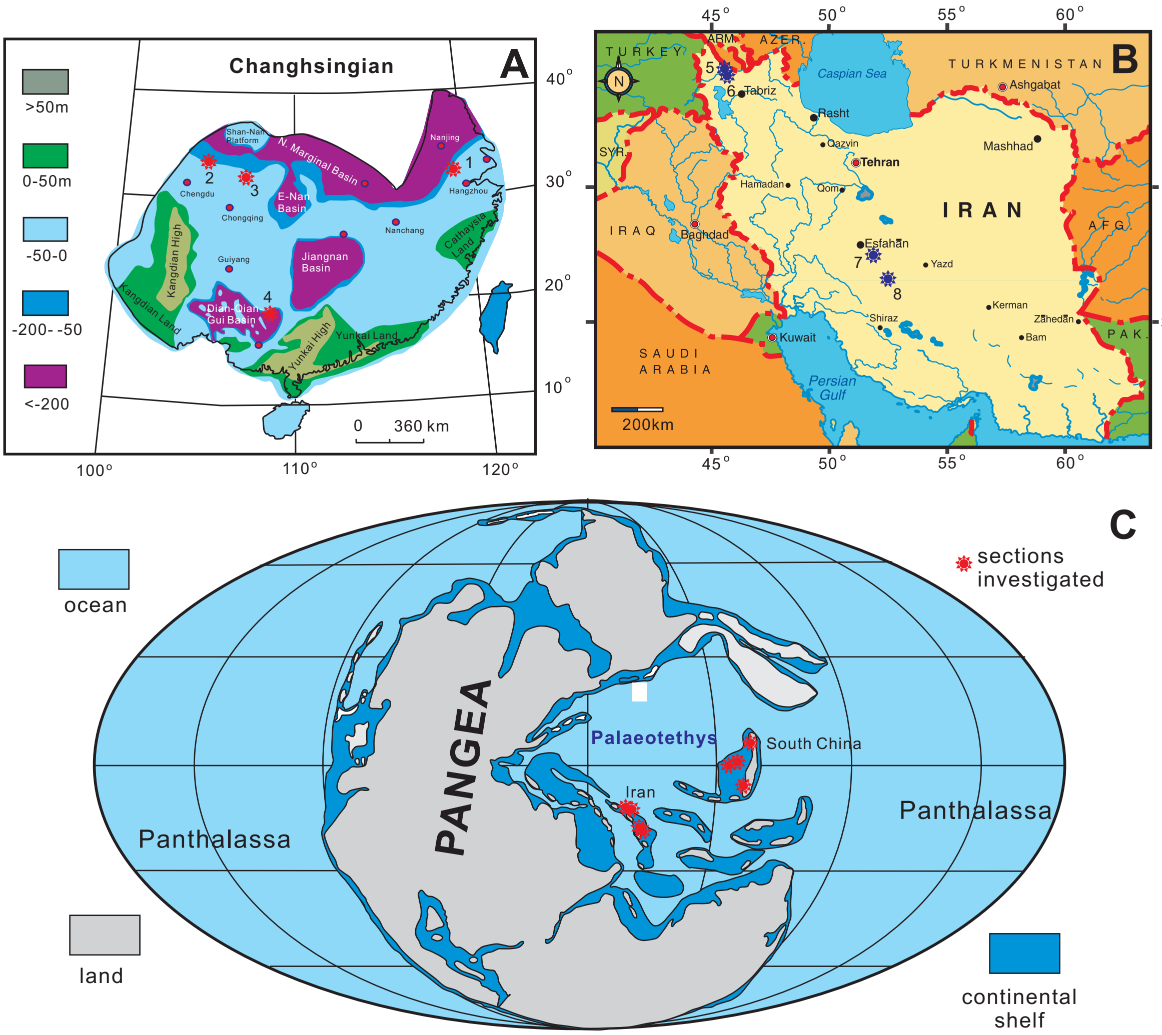

This is an author-produced, peer-reviewed version of this article. The final, definitive version of this document can be found online at *Earth and Planetary Science Letters*, published by Elsevier. Copyright restrictions may apply. DOI: 10.1016/j.epsl.2013.05.020.

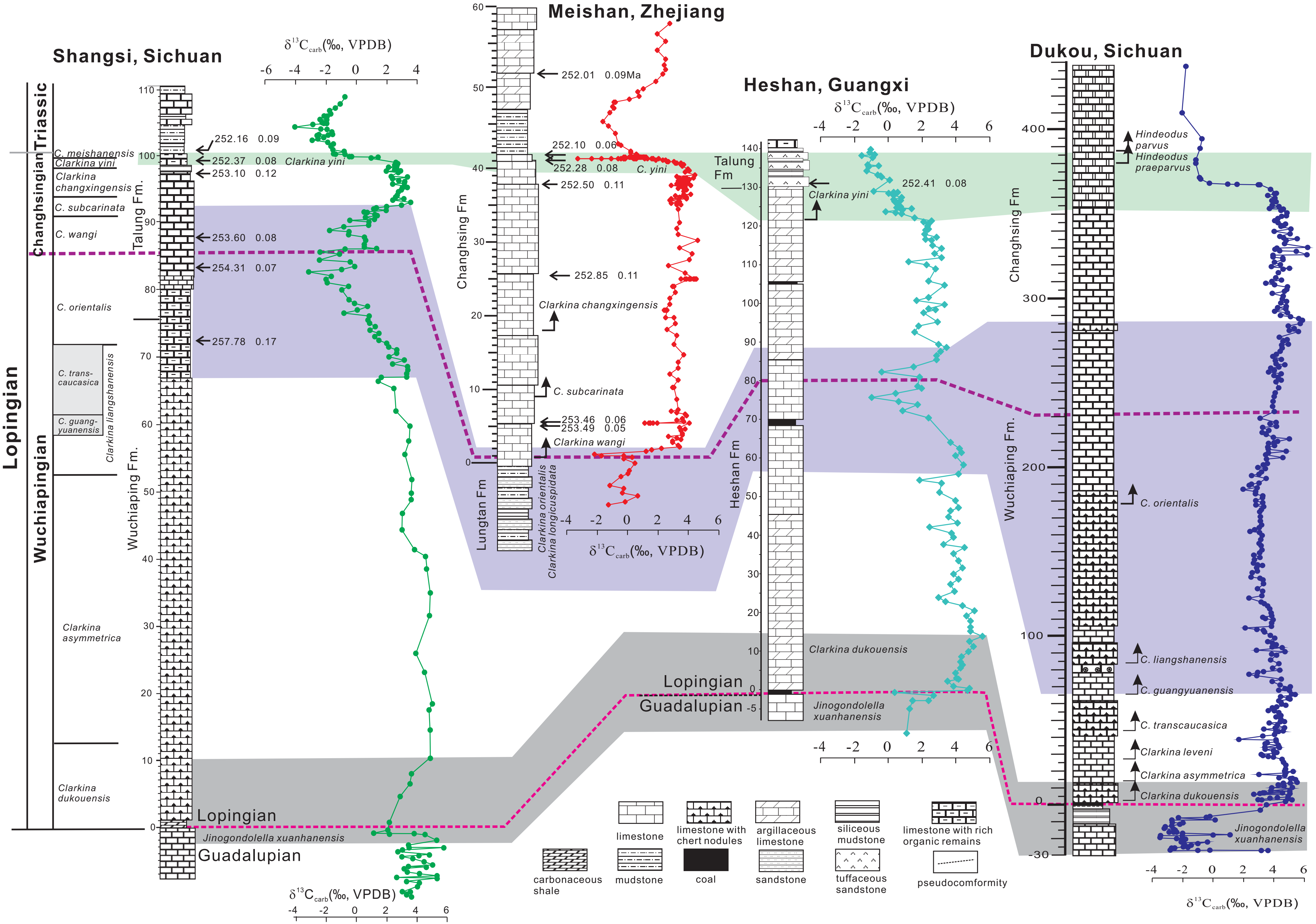

This is an author-produced, peer-reviewed version of this article. The final, definitive version of this document can be found online at *Earth and Planetary Science Letters*, published by Elsevier. Copyright restrictions may apply. DOI: 10.1016/j.epsl.2013.05.020.

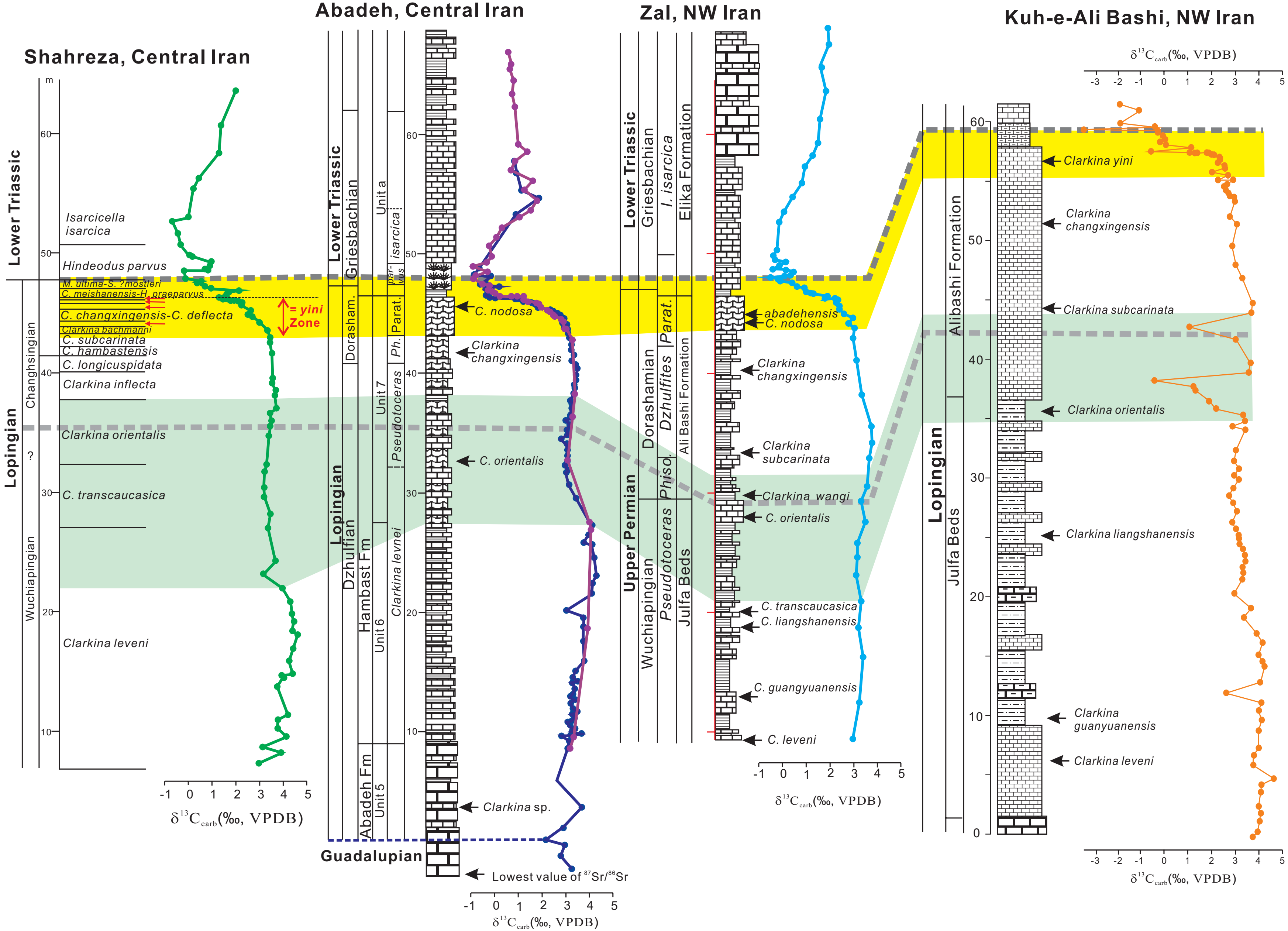

This is an author-produced, peer-reviewed version of this article. The final, definitive version of this document can be found online at *Earth and Planetary Science Letters*, published by Elsevier. Copyright restrictions may apply. DOI: 10.1016/j.epsl.2013.05.020.